A. Vantomme[1],
M.F. Wu[2]
G. Langouche

# The Formation of Surface and Buried Co-Silicides

## I. Introduction

In recent years, Co-silicides have been the object of very intensive studies [1-11]. A substantial amount of effort has especially been devoted to the investigation of $CoSi_2$. Both surface and buried layers of $CoSi_2$ have been of interest for applications in microelectronics, due to their high thermal stability, their very low resistivity (15-20 μΩcm at room temperature) and their small lattice mismatch to Si (only 1.2 %). Thin surface layers are very interesting as low resistance contact layers to Si. Buried layers, on the other hand, being semiconductor-metal-semiconductor (SMS) structures, are attractive for novel device applications, such as metal base transistors and three-dimensional devices [12-14].

Surface silicide layers can be obtained by furnace annealing of Co-covered Si single crystals, by annealing of high dose Co-implanted Si single crystals, by molecular beam epitaxy (MBE), by ion beam mixing (IBM). The first example of a buried Co-silicide layer was realized by a two step epitaxial growth of a $CoSi_2$ and a Si layer sequentially on a Si substrate with MBE [4]. White *et al* [5] first successfully synthesized a heteroepitaxial $Si/CoSi_2/Si$ structure by high dose Co implantation in a Si substrate (IBS : ion beam synthesis), resulting in monocrystalline buried $CoSi_2$ layers with sharp interfaces and with better electrical transport properties than those grown by more conventional techniques. In most cases, implantation energies around 200 keV are used. The lowest energy used is 100 keV [6, 7]. From the point of view of applications, it is more interesting to use thinner buried $CoSi_2$ layers [12]. Thinner films can be obtained by lowering the implantation energy. However, owing to the higher sputtering yield and the smaller projected range when using lower implantation energies, one might from surface $CoSi_2$ layers instead of buried layers. Moreover, to be suitable for applications, the thermal stability of these layers should be investigated in detail.

In principle, if the thickness of the epitaxial $CoSi_2$ layer is below a critical value $t_c$, the lattice mismatch will be completely accommodated by elastic strain and the epitaxial growth will be pseudomorphic. Otherwise, the lattice mismatch will be partially accommodated by the strain and partially by misfit dislocations near the interface. We used channeling spectroscopy and X-ray rocking curve measurements to determine the strain in our samples.

Another interesting phenomenon to be studied is the orientation of epitaxial silicide layers. Two orientations can exist on Si<111> : type A, which has exactly the same orientation as the substrate, and type B, which is rotated by 180° about the surface normal <111> axis. It has been checked what type of orientation can be obtained by implantation technique, and how this orientation can depend on the $CoSi_2$ layer thickness.

To investigate these silicide/silicon structures, several techniques have been combined, such as Rutherford backscattering spectroscopy - RBS - (relative composition, interface abruptness, layer thicknesses), channeling spectroscopy (crystalline quality, strain, orientation), cross section transmission electron microscopy - TEM - (crystalline quality, interface abruptness, layer thicknesses, orientation), electrical measurements (resistivity, thermal stability), X-ray rocking curve measurements (strain, orientation). These techniques, which give a more macroscopic (averaged in space) information, were combined with Mössbauer spectroscopy, a method which gives a more local (microscopic) information, and thus can distinguish between different chemical phases.

## II. Experimental

All Mössbauer spectra were measured at room temperature, using a single line absorber of 0.5 or 1.0 mg/cm² $^{57}Fe$ SFC (sodium ferrocyanide). The isomer shifts values were converted to absorber isomer shifts relative to α-iron.

A 2 MeV $He^+$ beam produced by a 5SHD-2 Pelletron is used for the RBS and channeling measurements with normal scattering geometry. To improve the depth resolution, glancing-angle geometry was sometimes used as well.

The resistivity measurements are carried out with a standard four-point-probe technique. The probes are formed by thin (30 μm diameter) Al alloy (99 % Al + 1 % Si) wires which are mounted on the sample with an Ultrasonic Wire Bounder. Measurements are made down to 0.5 K in a conventional $^3He$ resistivity cryostat. For the high-temperature measurements ($10 < T < 300$ K), a $^4He$ flow cryostat is used.

The X-ray rocking curve measurements were done with a computer-controlled 12 kW rotating anode Rigaku DMax II system, equipped with a flat pyrolytic carbon monochromator, and using a $CuK_\alpha$ (λ = 1.5418 Å) source. All the diffraction spectra were measured with a divergence slit of 1/6°, a receiving slit of 0.3 mm and a scattering slit of 1.2°. Typical counting times were between 1 and 20 seconds, stepping intervals were always 0.01° 2θ.

## III. Results and discussion

### *III.1. Surface silicide layers by annealing of Co-covered Si*

Surface Co-silicide layers were formed by furnace annealing (for 1 hr under $H_2$) of Co-covered Si single crystals. An 80 nm thick

*Instituut voor Kern - en Stralingsfysika, University of Leuven, B-3001 Leuven, Belgium.*
[1] *Research Assistant, NFWO (National Fund for Scientific Research, Belgium).*
[2] *On leave from the Peking University, Beijing, China.*

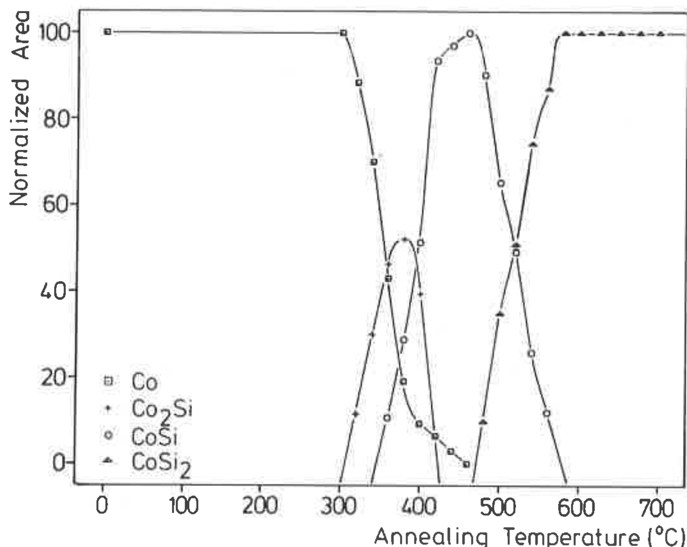


FIGURE 1. - *The normalized area of the various components in the formation of Co-silicide surface layers on Si as a function of annealing temperature, as deduced from the Mössbauer spectra.*

Co-layer was magnetron sputtered onto a Si<100> substrate. $^{57}Co$ was then implanted with a total dose of $3 \times 10^{14}$ atoms/cm$^2$ and an energy of 80 keV. This gives rise to an implantation range of about 24 nm, with a width of 16.5 nm [15]. The Mössbauer spectra are therefore representative for the behavior of the Co-layer.

After each annealing step of the Co-covered Si sample, we compared the obtained Mössbauer spectrum with the known [16] spectra of the various Co-silicides. *Figure 1* compiles the results of all our spectra. It shows that after annealing at temperatures up to 300 °C, no silicides are formed yet, resulting only in a magnetically split spectrum of $^{57}Fe$ in Co, with a magnetic field of 318(3) kG. From the relative amplitudes of the lines, we calculated $\theta = 86° 42'$ ($\theta$ is the angle between the magnetic field and the gamma ray direction, normal to the sample). Thus, there is a strong preferential magnetization along the plane, as can be expected for thin films. After annealing at higher temperatures (up to 900 °C), $Co_2Si$, CoSi and $CoSi_2$ are formed subsequently. It is a remarkable fact that two different Co-silicides can grow simultaneously : between 350 °C and 425 °C $Co_2Si$ and CoSi coexist, and between 475 °C and 575 °C CoSi and $CoSi_2$ are formed together. This phenomenon has only been observed for two transition metal silicides, namely for Co and Pt [2].

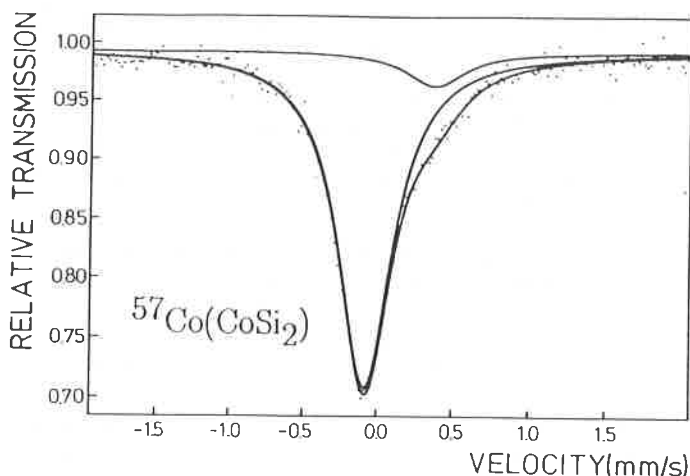


FIGURE 2. - *$^{57}Fe$ Mössbauer spectrum of a source of $^{57}Co$ implanted in $CoSi_2$ versus a single-line $^{57}Fe$-in-ferrocyanide absorber. For easy comparison with fig. 7, we have changed the sign of the velocity scale as if it were an absorber experiment.*

RBS measurements were performed simultaneously and confirmed fully our temperature dependent Mössbauer study. These RBS-data further show that the various silicide layers are formed in parallel layers on top of the Si-substrate. A more detailed study of these surface layer experiments is given in [17].

A surprising observation is that, although $CoSi_2$ has a cubic lattice ($CaF_2$) and thus is expected to give rise to a single line Mössbauer spectrum, we always find a broad side resonance next to the dominating single line *(Fig. 2)*, the origin of which is not completely understood. Some possible interpretations will be discussed further (§ III.3).

## *III.2. Buried and surface $CoSi_2$ layers by ion implantation*

### *The formation of buried and surface $CoSi_2$ layers by ion implantation*

Si <111> samples are implanted with Co ions with implantation energies of 30, 50, 70 and 160 keV in a temperature range from 300 °C to 400 °C and a vacuum of $10^{-6}$ Torr. In order to from a buried and continuous $CoSi_2$ layer, the doses are chosen to be slightly larger than their critical values [6, 7]. To form surface $CoSi_2$ layers, implantations are performed with doses about twice the values used for buried layers. For Mössbauer spectroscopy studies, the ion beam consisted of $^{59}Co$, alternated with small fractions (< 1 %) of $^{57}Co$.

A two-step annealing process, normally 600 °C for 1 hr followed by 1 000 °C for 1/2 hr is used to form the layers. Generally, we used conventional furnace annealing with an ambient of flowing $N_2/H_2$ ($H_2 \sim 25$ %) gas. In some cases rapid thermal processing in a $N_2$ ambient is also used.

As an example, we consider a sample which was implanted with $0.9 \times 10^{17}$ Co/cm$^2$ at 70 keV. The Mössbauer spectrum of the as-implanted sample at 350 °C contains lines of various silicides, formed after implantation. The dominant single line at relative velocity v = $-0.09(5)$ mm/s indicates that most of the Co has reacted with Si by forming precipitates with a local stoichiometry similar to $CoSi_2$. However, the resonances at positive velocity side show the existence of other local phases as well ($Co_2Si$, CoSi, interstitial Co, ...).

The RBS spectrum shows a Co-implantation profile with a nearly Gaussian shape, and a Co-peak concentration of only 22 %, which is not enough to form a continuous (macroscopic) $CoSi_2$ layer. The rather high minimum yield of the aligned spectrum ($\chi_{min}$ = 50 %) indicates that the sample is still heavily damaged. Combining these channeling results with those of the Mössbauer measurements, we can conclude that after implantation, microscopic precipitates of various silicides are formed, the largest part being $CoSi_2$.

The spectrum taken after annealing at 600 °C is the same as in the case of surface $CoSi_2$-layers on Si *(Fig. 2)*, which means that we have the same kind of anomaly as in the former case. The RBS spectrum confirms the occurrence of a buried continuous $CoSi_2$ layer. However, when we measure in channeling geometry, it is found that the minimum yield $\chi_{min}$ = 25 %, indicating that a good quality single crystal is not yet obtained. Only after annealing at 1 000 °C, the $\chi_{min}$ drops to 5 % *(fig. 3)*. Considering this enormous improvement of the crystalline quality, it is a surprising fact that the Mössbauer spectrum doesn't change at all : the same type of spectrum as in *figure 2* is obtained. This final improvement is therefore mainly long range reordering whereas the short range configuration, probed by Mössbauer spectroscopy, does not change any more.

*Table I* summarizes the results of various implantation energies. It shows that with lower energies, it is still possible to form continuous $CoSi_2$ layers, buried under a Si top layer (even with an implantation energy as low as 30 keV).

A cross section TEM picture corroborates that finally, after the

TABLE I. - *Epitaxial $CoSi_2$ layer identifications, preparation conditions and properties.*

| Sample | Condition of preparation | Annealing | Surface or buried | $\chi_{min}$ (%) | Thickness (nm) | $\Delta\Psi$ ($\pm$ 0.03°) | $\varepsilon_x^{\perp}$ ($\pm$ 0.03 %) | Type A (%) |
|---|---|---|---|---|---|---|---|---|
| 1 | SPE grown at 650 °C | 950 °C, 30' + 1 000 °C, 30' | Surface | 8 | 54 | 0.24° | – 1.66 % | 1.6 |
| 2 | $0.47\times10^{17}$ Co/cm² 30 keV at 300 °C | 600 °C, 60' + 1 000 °C, 30' | Buried | 3 | 20 | 0.31° | – 1.90 % | 30 |
| 3 | $0.58\times10^{17}$ Co/cm² 40 keV at 300 °C | 600 °C, 60' + 1 000 °C, 30' | Buried | 3 | 24 | 0.30° | – 1.87 % | 87 |
| 4 | $0.86\times10^{17}$ Co/cm² 70 keV at 310 °C | 600 °C, 60' + 1 000 °C, 30' | Buried | 3 | 36 | 0.30° | – 1.82 % | 99.6 |
| 5 | $1.40\times10^{17}$ Co/cm² 50 keV at 300 °C | 600 °C, 60' + 1 000 °C, 30' | Surface | 3 | 47 | 0.30° | – 1.87 % | 99.8 |
| 6 | $0.94\times10^{17}$ Co/cm² 30 keV at 300 °C | 600 °C, 60' + 1 000 °C, 30' | Surface | 6 | 36 | 0.31° | – 1.90 % | 100 |

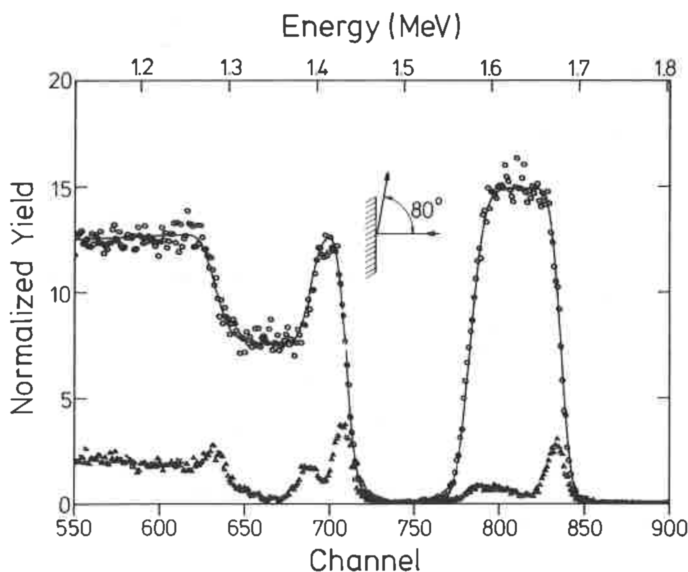


FIGURE 3. - *RBS spectra of a buried $CoSi_2$ layer, after annealing at 1 000 °C. • random ; + aligned ; – RBS simulation.*

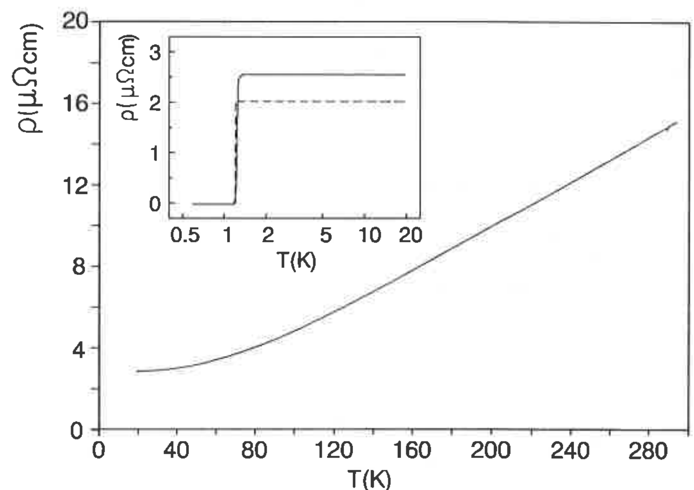


FIGURE 4. - *Temperature dependence of the resistivity of a buried $CoSi_2$ layer formed by implantation. Insert : $T_c$ of the buried layer.*

two step annealing, we obtain a monocrystalline and continuous buried layer with sharp interfaces (the interface roughness is estimated to be only about 15 Å).

The resistivity ϱ of $CoSi_2$ at room temperature is 15-20 μΩcm which is much lower than that of $Co_2Si$ and CoSi, so the resistivity measurements is also helpful to identify the phase of the buried layer. The ϱ(330 K) value of 15.5 μΩcm and a residual resistance ratio ϱ(300 K)/ϱ(4.2 K) of 5.4 indicate that this buried layer is a $CoSi_2$ layer with good electrical transport properties *(Fig. 4)*. In addition, the superconducting transition temperature $T_c$ of this buried $CoSi_2$ layer is measured (full line in the insert of *Fig. 4*) and, for comparison, of another surface $CoSi_2$ layer (dotted line) prepared by MBE. They are 1.3 K and 1.25 K respectively and are comparable with the results from others [5, 11].

### *Thermal stability of buried and surface $CoSi_2$ layers by ion implantation*

*Figure 5* shows the RBS spectra of three Co-implanted Si samples (50 keV with a dose of 0.6 × $10^{17}$ Co/cm²). It shows that the sample after 1 000 °C has a buried layer with abrupt interfaces *(Fig. 5a)*. Moreover, TEM *(Fig. 5B)* confirmed that a monocrystalline and continuous layers was formed. *Figure 5c* shows the RBS spectrum of another buried $CoSi_2$ layer, subsequently annealed at 1 100 °C for 30 min. In comparison with *figure 5a*, now the Co peak is lower and a tail is obvious, meaning that this annealing starts to change the Co profile of the sample. The corresponding TEM picture *(Fig. 5d)* shows that the interfaces are no longer as flat as after 1 000 °C annealing, and that voids are observed extending both above and below the buried silicide layer. The formation mechanism of the voids is still unclear. Finally, annealing at 1 200 °C for 5 min changes the Co profile significantly *(Fig. 5e)* and the TEM picture *(Fig. 5f)* shows that the continuous layer is broken up into islands distributed on top of the silicon substrate.

A similar study was done for surface $CoSi_2$ layers formed by ion implantation, and it was found that this kind of layer already breaks up into islands after 30 min annealing at 1 100 °C. Even more, the fact that the layer is broken up changes the resistivity as a function of temperature completely *(Fig. 6)*. Not only ϱ(300k) has increased by about three orders of magnitude, but it also shows a rather complicated electrical behavior instead of a simple metallic one. This layer now has both semiconductor and

FIGURE 5. - *RBS spectra and cross-sectional TEM pictures.* **(a,b)** *The buried* $CoSi_2$ *layer after annealing at 1 000 °C.* **(c,d)** *The buried* $CoSi_2$ *layer after further annealing at 1 100 °C for 30 min.* **(e,f)** *The broken-up* $CoSi_2$ *layer after annealing at 1 200 °C for 5 min.*

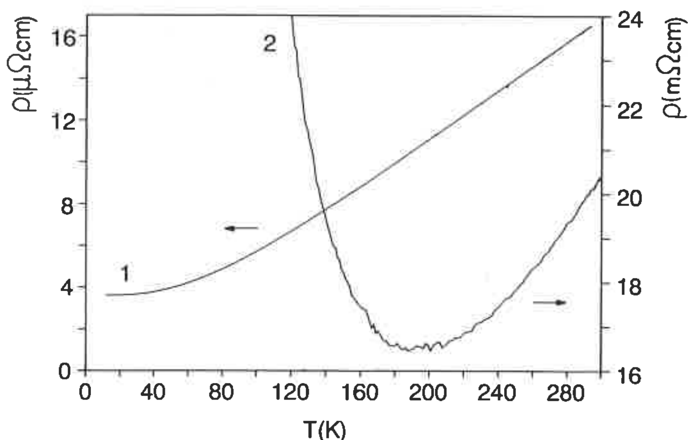


FIGURE 6. - *Temperature dependence of resistivity of a surface layer formed by implantation before (curve 1) and after (curve 2) annealing at 1 100 °C for 30 min.*

metallic electrical properties : at temperatures higher than 200 K the metallic behavior is more pronounced, whereas at temperatures lower than 200 K the semiconductor electrical behavior is dominant. Measurements on a high temperature annealed MBE $CoSi_2$ sample [18] showed similar results as in the case of an ion implanted surface sample, confirming the conclusion that buried $CoSi_2$ layers have a better thermal stability than a surface $CoSi_2$ layer.

### *III.3. Comparison of $^{57}Fe$ in $CoSi_2$ after direct ion implantation and after ion implantation of a radioactive parent*

Highly pure MBE-grown $CoSi_2$ was implanted with $3\times10^{15}$ $^{57}Fe$ atoms/cm$^2$ at 40 keV with the target kept at 300 °C. A target from the same MBE-grown sample was implanted under the same conditions with $^{57}Co$ with $1\times10^{15}$ atoms/cm$^2$. We compared the emission Mössbauer spectrum of the $^{57}Co$ source with the

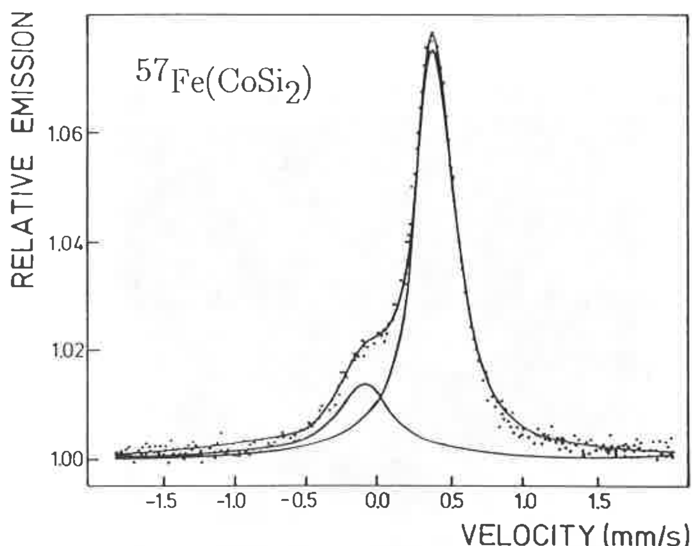


FIGURE 7. - *$^{57}Fe$ Mössbauer spectrum of an absorber of $^{57}Fe$ implanted at 300 °C into MBE-grown $CoSi_2$, using a single-line $^{57}Co$-in-Cu source.*

absorption spectrum (using a $^{57}Co$ in Cu single line source) of the $^{57}Fe$ target, measured by conversion electron Mössbauer spectroscopy.

*Figures 2* and *7* show the Mössbauer spectra of the $^{57}Co$ and $^{57}Fe$ implanted MBE-grown samples, respectively. Both spectra can be fitted with the same set of parameters. The two observed resonances have isomer shifts of $\delta_1 = -0.09(5)$ mm/s and $\delta_2 = +0.41(5)$ mm/s respectively. The striking observation is that, whereas almost all $^{57}Fe$ atoms after $^{57}Fe$ implantation are found with isomer shift $\delta_2$, almost all $^{57}Fe$ atoms after $^{57}Co$ implantation are found with isomer shift $\delta_1$.

In the case of $^{57}Co(CoSi_2)$, the dominating Mössbauer resonance *(Fig. 2)* with isomer shift $\delta_1$ is considered to be due to $^{57}Fe$ in the decay of $^{57}Co$ on regular Co lattice sites in cubic $CoSi_2$ [4-6]. The origin of the second resonance is much harder to account for. Its isomer shift is close to the value measured for CoSi, but careful X-ray analysis could not detect any crystalline trace of this place. It cannot even be associated with the implantation process as it also appears after diffusion in bulk $CoSi_2$.

We can tentatively propose two interpretations for this anomalous resonance :

1 - It is associated with $^{57}Fe$ atoms in the decay of $^{57}Co$ atoms in a lattice configuration which is different from the normal substitutional Co atoms in $CoSi_2$. As the electron density at the $^{57}Fe$ nucleus is close to the one observed in CoSi, a local deviation from the correct stoichiometry towards a more Co-rich one can be responsible for this.

2 - The $^{57}Co$ parent atoms are found in a correct $CoSi_2$ stoichiometry, but an anomalous charge state is stabilized at least during the 200 nanosecond lifetime of the excited Mössbauer state of $^{57}Fe$.

When the $^{57}Fe$ isotope is implanted rather than $^{57}Co$, it is a surprising observation to discover *(Fig. 7)* that a large majority of $^{57}Fe$ is found with the same hyperfine interaction parameters as the anomalous resonance of the $^{57}Co$ implantations. So far we do not have extensive data on different types of $CoSi_2$ implanted with $^{57}Fe$, so that we cannot make a full comparison under different conditions. The present observations can somehow fit in both proposed interpretations for $^{57}Co$ :

1 - During the final relaxation phase of the collision cascade, it can not be excluded that an impurity atom like Fe preferentially ends up in a different local stoichiometric surrounding than (a Co atom in a) regular $CoSi_2$. What we then observe is that the local (Co-rich ?) configuration which is preferred by the majority of the Fe atoms is the same as the one preferred by a minority of the Co atoms.

2 - If the two isomer shifts are due to different electronic configurations in the same stoichiometric $CoSi_2$, we have to conclude that both are very stable, and that Fe atoms that have been implanted and came to rest long before the Mössbauer experiment prefer a different electronic configuration than the Fe atoms that came into existence only nanoseconds before the Mössbauer experiments.

## *III.4. Strain and orientation in epitaxial $CoSi_2$ (111) layers formed by ion implantation*

The disilicides $NiSi_2$ and $CoSi_2$ have the cubic $CaF_2$ structure with a lattice mismatch of $-0.46$ % and $-1.2$ % with respect to Si respectively. The misalignment (or kink angle) $\Delta\Psi$ between the relevant axes in the epilayer and in the substrate is a direct measure for the tetragonal distorsion $\varepsilon_T$ caused by the strain :

$$\varepsilon_T = \varepsilon_r^{\parallel} - \varepsilon_r^{\perp} = \Delta\Psi / (\sin\Psi \cos\Psi) \quad (1)$$

where $\varepsilon_r^{\parallel}$ and $\varepsilon_r^{\perp}$ are the two components defined relative to $d_{LF}$ (the interplanar spacing of the layer material under free lattice conditions) : $\varepsilon_r^{\perp} = (d_L^{\perp} - d_{LF})/d_{LF}$ and $\varepsilon_r^{\parallel} = (d_L^{\parallel} - d_{LF})/d_{LF}$. $d_L$ is the spacing of the strained layer. On the other hand, when defined relative to $d_S$, the substrate spacing, $\varepsilon_X^{\perp} = (d_L^{\perp} - d_S)/d_S$ and $\varepsilon_X^{\parallel} = (d_L^{\parallel} - d_S)/d_S$ are used. More detailed explanations concerning these components and how they can be measured by channeling spectroscopy or by X-ray rocking curve measurements, are given in [19-23]. According to the definition, it is clear that for a totally coherent or pseudomorphic $CoSi_2$ layer on a Si substrate, the parallel strain should have a value $\varepsilon_r^{\parallel} = 1.2$ %. This is the case if the epitaxial layer has not reached its critical thickness $t_c$. Concerning $t_c$, two theoretical models [24, 25] have been developed. Although the predicted $t_c$ values differ by two orders of magnitude, both models are claimed to be supported by experiments [26].

In the case of epitaxial $CoSi_2$ (111) layers prepared by IBS, few strain studies have been performed and the results are more consistent than the data obtained on UHV $CoSi_2$ layers. For implanted layers with thicknesses in the order of 100 nm, a perpendicular strain $\varepsilon_X^{\perp} = -1.68$ % was found, which is smaller than $-3.5$ %, the value expected for a completely strained layer [27-28]. As we were able to form $CoSi_2$ layers as thin as 20 nm by ion implantation, we can study whether our thinner layers have a larger strain or tetragonal distortion or whether they are closer to pseudomorphic growth.

The orientation of epitaxial silicide layers is another interesting phenomenon to be studied. Two orientations exist on Si (111) : type A silicide has the same orientation as the substrate, while type B silicide is rotated 180° about the surface normal <111> axis. Unlike for $NiSi_2$, where the orientation can be controlled, for $CoSi_2$ layers prepared by UHV procedures on a Si (111) substrate, the type B orientation is always predominant [29]. On the contrary, $CoSi_2$ layers with a type A orientation can easily be grown by IBS. The questions whether the $CoSi_2$ layers formed by IBS have always the pure type A orientation, and whether the strain in the $CoSi_2$ layers will be related with its orientation, as is the case for $NiSi_2$ layers [30], will be studied.

### *Strain*

The preparation conditions and some properties of the six epitaxial $CoSi_2$ samples (1-6) are compiled in *Table I*. With the exception of sample 1, all samples are prepared by ion implantation followed by two step annealing. RBS/channeling and X-ray rocking curve measurements enable to determine the strain and orientation of the epilayers in these samples.

*Figures 8* and *9* show the angular scans for the different layers of two samples which contain a surface (sample 5) and a buried (sample 4) $CoSi_2$ layer respectively. The scans were made around the <114> axis (left) and the <110> axis (right) in the ($1\bar{1}0$) plane of the Si substrate. The angle between the <114> and <110> axes of the Si substrate is $2\Psi = 70.52$°, indicating that the

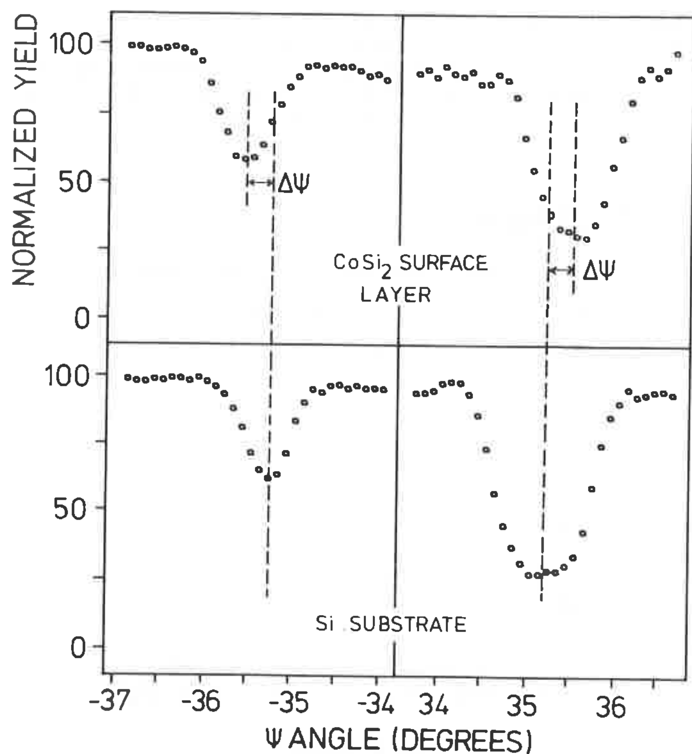


FIGURE 8. - *Angular scan around the <114> (left) and <110> (right) axes in the (1$\bar{1}$0) plane of sample 5.*

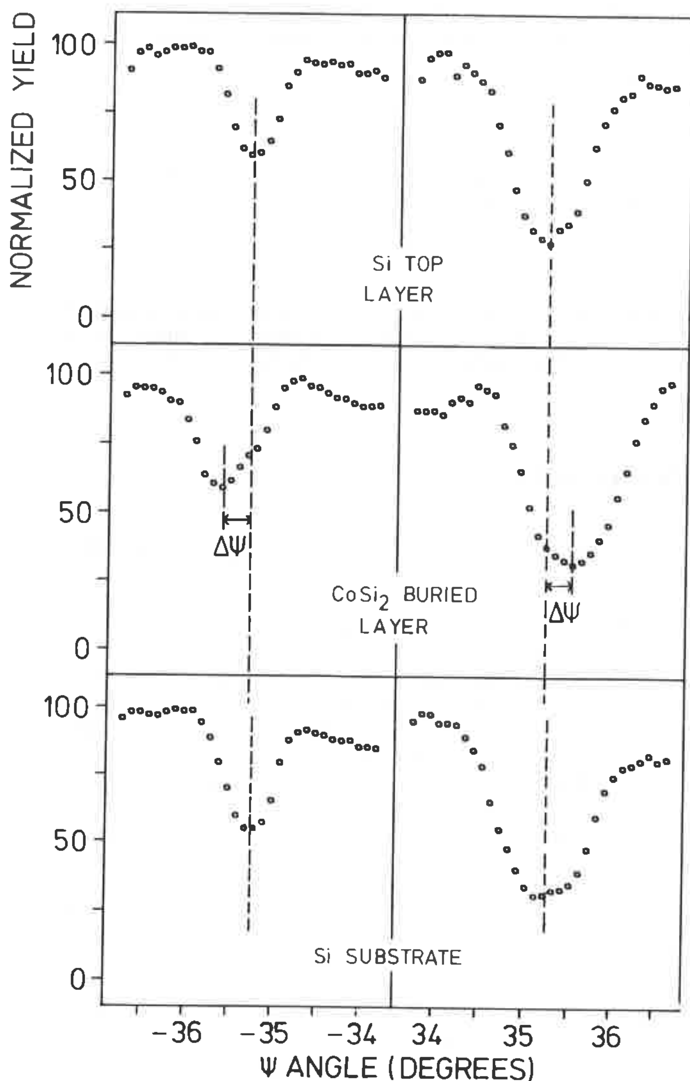


Si substrate is a perfect cubic single crystal free of strain. On the other hand, the angle between these two axes of the epilayer is $2\times(35.26 + \Delta\Psi)$ with $\Delta\Psi = 0.31° \pm 0.03°$ as shown in *Figures 8* and *9* and as listed in *Table I*. This result indicates that these epilayers are strained with a tensile strain parallel to the interface and a compressive strain perpendicular to the interface. Using eq.(1), a tetragonal distorsion $\varepsilon_T = (1.15 \pm 0.11)$ % can be deduced from the measured $\Delta\Psi$. From X-ray rocking curve measurements, the perpendicular strain was found to be $\varepsilon_r^{\perp} = -0.69$ %. With the assumption of volume conservation for the strained layer, a $\varepsilon_r^{\parallel}$ value of + 0.35 % can be deduced. Finally, a value of $\varepsilon_T = \varepsilon_r^{\parallel} - \varepsilon_r^{\perp} = (1.04 \pm 0.05)$ % is obtained, which agrees well with the $\varepsilon_T$ value calculated from the results of channeling measurements. As listed in *Table I*, the five ion implanted samples have rather close perpendicular strain values with an average $\varepsilon_X^{\perp}$ value of − 1.9 %, which is larger than in the SPE grown sample, although our epitaxial layers are still far from a completely strained or totally coherent layer.

The strain measurements could eventually be influenced by the steering effect of the $He^+$ beam, because some of the channeled ions can be steered into misaligned channels after crossing the interface. In contrast to the results of Kohlhof [27] and Barbour [8], we have no indication that our measurements are influenced by this steering effect. This is discussed in [22].

## *Orientation*

*Figures 8* and *9* show that when the angular scan is measured around the <114> axis of the Si substrate, the channeling dips from both the Si substrate and from the $CoSi_2$ surface and buried layer have the characteristics corresponding to the <114> axis, i.e. a higher $\chi_{min}$ value and a narrower width. On the oder hand, when the scan is around the <110> axis of the Si substrate, both channeling dips show the same characteristics of the <100> axis. This confirms that these $CoSi_2$ layers which are prepared by IBS have the same orientation as their Si substrate, indicating that their orientations are pure type A or predominantly type A. However, when the $CoSi_2$ layers become rather thin, they were found to contain a mixed A+B type with a comparable amount of both orientations. Because the RBS/channeling technique can not determine the relative amount of type A and type B accurately in an epitaxial layer with mixed A+B type, we applied X-ray rocking curve measurements which have a high sensitivity and accuracy for such orientation determination. The results are listed in the last column of *Table I* and *Figure 10*. It can be seen that even a very weak type B component of only 0.2 % (sample 5) can still clearly be detected.

If the relative amount of type A is set out as a function of layer thickness, a strong correlation is found *(Fig. 11)*. When the thickness decreases to 20 nm (sample 2), the relative amount of type B component can be as large as 70 %. Tung [31] pointed out that the dominance of type B orientation in the epitaxial silicide layers formed by UHV procedures can be attributed to its lower interface free energy so that the type B orientation in energetically favored. Unlike the UHV procedure, where the epitaxial $CoSi_2$ layer is grown layer by layer, the formation of $CoSi_2$ precipitates with different sizes in the Si substrate is the primary step in the IBS procedure. Bulle-Lieuwma [32] argued that the preferential growth of aligned precipitates causes the formation of continuous epitaxial layers with aligned (type A) orientation. Our results indicate that for thinner buried layers prepared by IBS, interface effects dominate over bulk effects, so that the preferential growth of type A precipitates is suppressed by the influence of the $CoSi_2$/Si interface, which seems to drive the system preferentially towards a type B orientation as shown in the layers grown by SPE (sample 1).

FIGURE 9. - *Angular scan around the <114> (left) and <110> (right) axes in the (1$\bar{1}$0) plane of sample 4.*

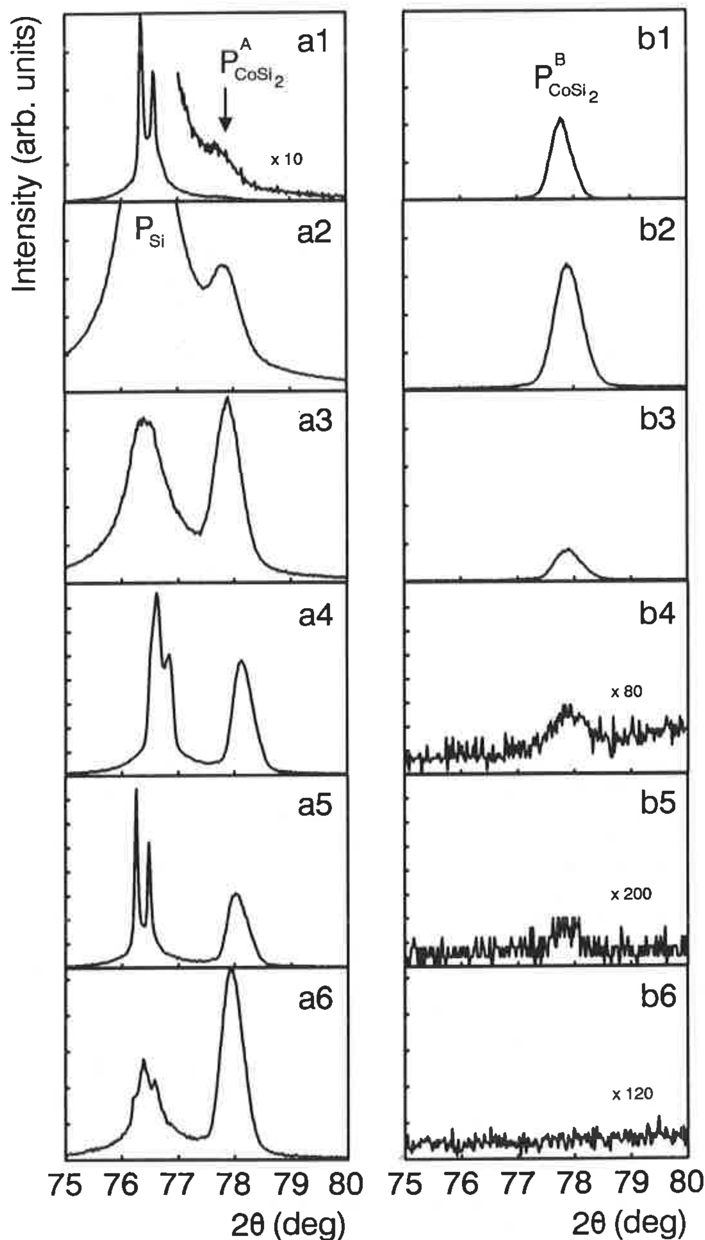


FIGURE 10. - *X-ray rocking curves around the* $<331>^A_{CoSi_2}$ *axis (a1-a6) and the* $<331>^B_{CoSi_2}$ *axis (b1-b6) from the respective samples of* Table I. *The corresponding a and b curves have the same intensity scale. The splitting of* $P_{Si}$ *and the asymmetry in* $P^{A,B}_{CoSi_2}$ *are due to the presence of* $K_{\alpha 1}$ *and* $K_{\alpha 2}$ *in the x-ray beam.*

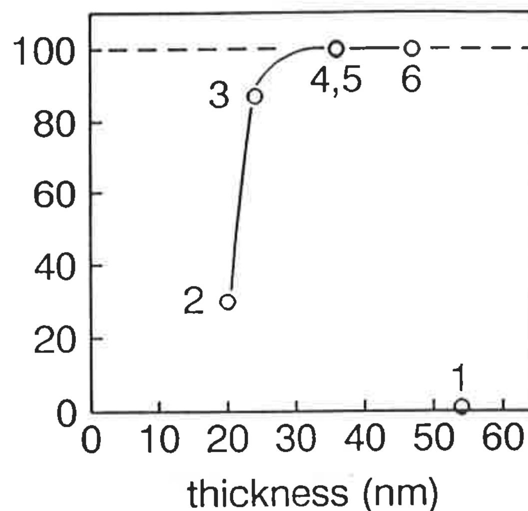


FIGURE 11. - *Relative amount of type A* $CoSi_2$ *prepared by IBS and SPE as a function of the* $CoSi_2$ *epilayer thickness. The labels refer to the sample identifications in* Table I. *The line is a guide to the eye.*

## Conclusion

Mössbauer spectroscopy, complemented with RBS and channeling spectroscopy, has shown that after annealing of Co surface layers on Si, $Co_2Si$, CoSi and $CoSi_2$ are formed subsequently in parallel layers on the Si substrate. When Co is implanted in Si, buried and surface $CoSi_2$ layers can be formed after annealing at 600 °C. The best crystalline quality is reached after 1 000 °C annealing, as confirmed also by TEM. Our study has further shown that different hyperfine interaction parameters are observed at Fe atoms that were directly implanted into $CoSi_2$, and Fe atoms that were formed due to the radioactive decay of implanted $^{57}Co$ atoms. Finally, a combination of RBS/channeling and X-ray rocking curve measurements showed that our $CoSi_2$ layers prepared by IBS are strained ($\varepsilon^{\perp}_{X}$ = − 1.9 %) more than the thicker IBS-formed layers or MBE grown layers, but the values are still much lower than $\varepsilon^{\perp}_{X}$ = − 3.5 % for a totally coherent layer. Epitaxial $CoSi_2$ (111) layers with pure type A or predominant type A orientation can easily be formed by IBS. However, a component of type B appears if the thickness of the epilayer decreases to less than 36 nm, an reaches a relative amount of 70 % for a layer with a 20 nm thickness.

*Acknowledgments :* This work was supported by the Belgian IIKW and GOA (Government Concerted Action) projects. The authors would also like to thank J.M. Phillips for providing the MBE-samples.

## References

[1] S.S. Lau, J.W. Mayer, K.N. Tu, *J. Appl. Phys.*, **1978**, *49*, 4005.
[2] G.J. van Gurp, C. Langereis, *J. Appl. Phys.*, **1975**, *46*, 4301.
[3] K.N. Tu, G. Ottoviani, R.D. Thompson, J.W. Mayer, *J. Appl. Phys.*, **1982**, *53*, 4406.
[4] R.T. Tung, J.M. Poate, J.C. Bean, J.M. Gibson, D.C. Jacobson, *Thin Solid Films*, **1982**, *93*, 77.
[5] A.E. White, K.T. Short, R.C. Dynes, J.P. Garno, J.M. Gibson, *Appl. Phys. Lett.*, **1987**, *50*, 95.
[6] A.E. White, K.T. Short, R.C. Dynes, J.M. Gibson, R. Hull, *MRS Symp. Proc.*, **1988**, *100*, 3.
[7] K. Kohlhof, S. Mantl, B. Stritzker, W. Jager, *Nucl. Inst. Methods B*, **1989**, *39*, 276.
[8] J.C. Barbour, S.T. Picraux, B.L. Doyle, *MRS Symp. Proc.*, **1988**, *107*, 269.
[9] A.H. van Ommen, W.F.J. Slijkerman, K. Nakagawa, R.J. Smith, J. van der Veen, C.W.T. Bulle-Lieuwma, *J. Appl. Phys.*, **1988**, *64*, 3005.
[10] S.P. Murarka, Silicides for VLSI applications, Academic Press, New York, **1983**.
[11] M.-A. Nicolet, S.S. Lau, *in* "VLSI Electronics : Microstruc-

ture Science", Vol. 6 (M.G. Einspruch, G.B. Larrabee, eds.), Academic Press, New York, **1983**, Chap. 6.
[12] J.C. Hensel, A.F.J. Levi, R.T. Tung, J.M. Gibson, *Appl. Phys. Lett.*, **1985**, *47*, 151.
[13] J.C. Hensel, *MRS Symp. Proc.*, **1987**, *54*, 499.
[14] E. Rosencher, F. Arnaud d'Avitaya, P.A. Badoz, C. D'Anterroches, G. Glastre, G. Vincent, J.C. Pfister, *MRS Symp. Proc.*, **1987**, *91*, 415.
[15] J.F. Ziegler, J.P. Biersack, U. Littmark, *in* : The Stopping and Range of Ions in Mater (J.F. Ziegler, ed.), Pergamon, New York, **1985**, p. 202.
[16] I. Dézsi, H. Engelman, U. Gonser, G. Langouche, *Hyp. Int.*, **1987**, *33*, 161.
[17] A. Vantomme, I. Dézsi, G. Langouche, *Hyp. Int.*, **1988**, *41*, 725.
[18] M.F. Wu, A. Vantomme, H. Pattyn, G. Langouche, K. Maex, J. Vanhellemont, J. Vanacken, H. Vloeberghs, Y. Bruynseraede, *Nucl. Instr. Methods B*, **1990**, *45*, 658-663.
[19] H. Vanderstraeten, Y. Bruynseraede, M.F. Wu, A. Vantomme, G. Langouche, J.M. Phillips, accepted for publication in *Appl. Phys. Lett.,* **1990**, *57,* 135.
[20] H. Vanderstraeten, Y. Bruynseraede, M.F. Wu, A. Vantomme, G. Langouche, submitted to *J. Phys. D. : Appl. Phys.,* **1991**, *24,* 937.
[21] M.F. Wu, A. Vantomme, G. Langouche, K. Maex, J. Vanhellemont, to be publ. in the *Proc. of the 1st Intern. Conf. on Epit. Cryst.*, Growth, 1-7 April **1990**, Budapest, **1991**, *32-34,* 169.
[22] M.F. Wu, A. Vantomme, G. Langouche, J. Vanderstraeten, Y. Bruynseraede, *Nucl. Instr. Methods B.,* **1991**, *54,* 444.
[23] M.F. Wu, A. Vantomme, G. Langouche, K. Maex, H. Vanderstraeten, Y. Bruynseraede, *Appl. Phys. Lett.,* **1990**, *57,* 1973
[24] J.W. Matthews, A.E. Blakeslee, *J. Cryst. Growth*, **1974**, *27*, 118.
[25] R. People, J.C. Bean, *Appl. Phys. Lett.*, **1985**, *47*, 322 ; **1986**, *49*, 229.
[26] P.J. Orders, B.F. Usher, *Appl. Phys. Lett.*, **1987**, *50*, 980.
[27] K. Kohlhof, S. Mantl, B. Stritzker, *Appl. Surface Sci.*, **1989**, *38*, 207.
[28] A.H. van Ommen, J.J.M. Ottenheim, C.W.T. Bulle-Lieuwma, *Appl. Surface Sci.*, **1989**, *38*, 197.
[29] R.T. Tung, J.M. Gibson, J.C. Bean, J.M. Poate, D.C. Jacobson, *Appl. Phys. Lett.*, **1982**, *40*, 684.
[30] M. Okamoto, S. Hashimotot, B.D. Hunt, L.J. Schowalter, *Mater. Res. Soc. Symp. Proc.*, **1986**, *56*, 157.
[31] R.T. Tung, J.M. Gibson, *Mater. Res. Soc. Symp. Proc.*, **1986**, *67*, 211.
[32] C.W.T. Bulle-Lieuwma, A.H. van Ommen, L.J. van Ijzendoorn, *Appl. Phys. Lett.*, **1989**, *54*, 244.